



1 **Basin inversion and structural architecture as constraints on fluid**
2 **flow and Pb-Zn mineralisation in the Paleo-Mesoproterozoic**
3 **sedimentary sequences of northern Australia**

4

5 **George M. Gibson**, Research School of Earth Sciences, Australian National University, Canberra ACT
6 2601, Australia

7 **Sally Edwards**, Geological Survey of Queensland, Department of Natural Resources, Mines and Energy,
8 Brisbane, Queensland 4000, Australia

9 **Abstract**

10 As host to several world-class sediment-hosted Pb-Zn deposits and unknown quantities of conventional and
11 unconventional gas, the variably inverted 1730-1640 Ma Calvert and 1640-1580 Ma Isa superbasins of
12 northern Australia have been the subject of numerous seismic reflection studies with a view to better
13 understanding basin architecture and fluid migration pathways. Strikingly similar structural architecture
14 has been reported from much younger inverted sedimentary basins considered prospective for oil and gas
15 elsewhere in the world. Such similarities suggest that the mineral and petroleum systems in Paleo-
16 Mesoproterozoic northern Australia may have spatially and temporally overlapped consistent with the
17 observation that basinal sequences hosting Pb-Zn mineralisation in northern Australia are bituminous or
18 abnormally enriched in hydrocarbons. This points to the possibility of a common tectonic driver and shared
19 fluid pathways. Sediment-hosted Pb-Zn mineralisation coeval with basin inversion first occurred during the
20 1650-1640 Ma Riversleigh Tectonic Event towards the close of the Calvert Superbasin with further pulses
21 accompanying the 1620-1580 Ma Isa Orogeny which brought about closure of the Isa Superbasin.
22 Mineralisation in all cases is hosted by the syn-inversion fraction of basin fill, contrary to most existing
23 interpretations of Pb-Zn ore genesis where the ore-forming fluids are introduced during the rifting or syn-
24 extensional phase of basin development. Syn-extensional normal faults of Calvert and Isa age are mutually
25 orthogonal, giving rise to a complex compartmentalisation of sub-basins with predominantly NNW and
26 ENE strikes. Basin inversion subsequent to 1640 Ma occurred in a transpressive tectonic regime linked to
27 continent-continent collision accompanied by orogen-parallel extensional collapse and right-stepping
28 strike-slip faulting.

29 **Introduction**

30 Northern Australia and its late Paleoproterozoic-early Mesoproterozoic basinal sequences have long
31 attracted the interest of the minerals and petroleum exploration industries. Besides being the world's single
32 largest repository of sediment-hosted Pb-Zn mineral deposits (Huston et al., 2006; Southgate et al., 2006),
33 these same mineral-rich sequences hold some of the planet's oldest oil (Jackson et al., 1986) along with an
34 unknown quantity of conventional and unconventional gas (Carr et al., 2019; Gorton and Troup, 2018;
35 McConachie et al., 1993). Unsurprisingly, many mineral deposits and their host rocks are bituminous or
36 contain very high proportions of carbon (Andrews, 1998; Broadbent et al., 1998; Hutton and Sweet, 1982;
37 Jarrett et al., 2018; McConachie et al., 1993; McGoldrick et al., 2010), raising the possibility that the
38 petroleum and mineralising systems in northern Australia may have temporally and spatially overlapped
39 and share a common tectonic driver. Such a possibility was first entertained for the 1575 Ma Century Pb-
40 Zn deposit (Fig. 1a) where first hydrocarbons and then a more metalliferous ore-forming fluid are thought
41 to have been sequentially trapped following their expulsion from deeper stratigraphic levels during folding
42 and thrusting accompanying the 1620-1575 Ma Isan Orogeny (Broadbent et al., 1998). In this scenario,



43 basin inversion was not only intimately linked to fluid migration and mineralisation but played a key role
44 in generating the structural architecture that brought the petroleum and mineralising systems together in
45 one place. Seismic reflection images for the Lawn Hill Platform have since shown the Century deposit to
46 be hosted by the syn-inversion fraction of basin fill (Gibson et al., 2017; Gibson et al., 2016) and occur in
47 rocks possessing a structural architecture common to inverted basins the world over, including those
48 currently under exploration for oil and gas in the Irish and North seas and north European continental shelf
49 more generally (Cooper et al., 1984; Hayward and Graham, 1989; Lowell, 1995; Thomas and Coward,
50 1995; Turner and Williams, 2004). Thus, not only does basin inversion appear to have been a prerequisite
51 for ore formation at Century but the structural architecture cannot have appreciably changed during the
52 transition from a hydrocarbon to mineral system lest the similarities with their more modern European
53 counterparts have been lost during crustal shortening. Such conclusions are difficult to reconcile with most
54 existing models for sediment-hosted Pb-Zn mineralisation in northern Australia where ore formation is
55 interpreted to have been syn-extensional and facilitated by fluid migration along normal faults active at the
56 time of basin formation (Huston et al., 2006; Kunzmann et al., 2019; Large et al., 2005; Leach et al., 2010;
57 McGoldrick et al., 2010). Alternative exploration strategies for this and other types of sediment-hosted Pb-
58 Zn mineralisation in northern Australia may therefore be warranted that better reflect the similarities with
59 the petroleum system and target the structures formed during basin inversion. Here, we make use of
60 publically available industry and government deep seismic reflection data to show that inversion-related
61 structures of more than one generation and style are widely developed in the late Paleoproterozoic-early
62 Mesoproterozoic basin sequences of northern Australia (Figs. 1 & 2), reflecting successive episodes of
63 crustal shortening during the course of which the majority of Pb-Zn deposits were emplaced (Gibson et al.,
64 2017).

65 **Regional geology and basin-forming events of northern Australia**

66 Northern Australia's late Paleoproterozoic-early Mesoproterozoic basinal sequences belong to one of three
67 superbasins (Figs. 2 & 3) which, together with the overlying and younger South Nicholson Basin (Fig. 1a),
68 preserve a 300 Myr history of lithospheric extension interrupted by successive episodes of basin inversion,
69 uplift and erosion (Betts et al., 2006; Blake, 1987; Gibson et al., 2012; Giles et al., 2002; Jackson et al.,
70 2000; O'Dea et al., 1997b; Southgate et al., 2000a; Withnall and Hutton, 2013). The oldest basin inversion
71 event (Fig. 3) occurred subsequent to 1840 Ma and is best expressed by the angular unconformity separating
72 the 6-8 km thick 1790-1740 Ma Leichhardt Superbasin (Fig. 2) from an older underlying ≥ 1870 Ma
73 crystalline basement (Kalkadoon-Leichhardt Block; Fig. 2) variably intruded by foliated 1860-1840 Ma
74 granites (Blake, 1987; Withnall and Hutton, 2013). Clasts of strongly foliated granite and other basement
75 rocks occur widely in conglomerates at the base of the Leichhardt Superbasin (1790 Ma Bottletree
76 Formation) but otherwise its basin fill is only mildly deformed and metamorphosed, and mainly comprises
77 continental tholeiites and rhyolite interstratified with subordinate but still substantial volumes of fluvial-
78 shallow marine sedimentary rocks. This same cover-basement relationship is also evident on the Murphy
79 Ridge farther north where conglomerates (Westmoreland Conglomerate) at the base of the 1790-1740 Ma
80 Tawallah Group (Fig. 3) in the McArthur Basin (Fig. 1b) similarly rest unconformably on an older deformed
81 basement intruded by 1860-1840 Ma granites (Withnall and Hutton, 2013). As with the Kalkadoon-
82 Leichhardt Block, basement granites on the Murphy Ridge were deformed long before the overlying
83 conglomerate was deposited and likely represent exposed fragments of a much more regionally extensive
84 magmatic belt that is continuous at depth and once lay at or close to the eastern margin of the North
85 Australian Craton. Granites with calc-alkaline compositions occur widely throughout the Kalkadoon-
86 Leichhardt Block (Bierlein et al., 2011) and may originally have formed part of a continental magmatic arc
87 linked to west-dipping subduction beneath the eastern margin of the craton (Bierlein et al., 2008; Korsch et
88 al., 2012). Alternatively, these granites originated in a backarc setting linked to oceanward retreat of a more



89 distal arc built along either the southern or eastern margin of conjoined North and South Australian cratons
90 (Betts et al., 2016; Betts et al., 2008; Giles et al., 2002) or eastern margins (Gibson and Champion, 2019;
91 Gibson et al., 2018; Gibson et al., 2008). Regardless of which interpretation is correct, by 1790 Ma
92 lithospheric extension and thinning were well underway and northern Australia was subjected to
93 widespread intracontinental rifting, normal faulting and half-graben formation accompanied at deeper
94 crustal levels to elevated heat flow, low pressure-high temperature metamorphism and bimodal magmatic
95 intrusion (Betts et al., 2016; Betts et al., 2006; Gibson et al., 2012; Gibson et al., 2008; Giles et al., 2002;
96 Giles et al., 2004; Holcombe et al., 1991; O'Dea et al., 1997a; Pearson et al., 1991). Lithospheric extension
97 during this phase of basin formation produced mainly northwest-oriented normal faults and half-graben and
98 continued through until ca. 1740 Ma when backarc extension and rifting in the Mount Isa region and
99 neighbouring McArthur Basin (Fig. 1a) temporarily ceased and gave way to an episode of thermal
100 subsidence accompanied by the deposition of shallow marine quartzite and carbonate rocks (Gibson et al.,
101 2012; Jackson et al., 2000; O'Dea et al., 1997b) .

102 The Leichhardt Superbasin concluded in a period of renewed tectonic instability variously attributed to
103 onset of a 1730-1710 Ma orogenic event (Blaikie et al., 2017) or a renewal in fault-block rotation and tilting
104 (Gibson et al., 2012; Gibson et al., 2008). Either way, uplift and erosion accompanying this event resulted
105 in the formation of a deeply incised and regionally extensive angular unconformity above which
106 conglomerates and redbeds of the Bigie Formation were deposited (Fig. 3). Their deposition marks the start
107 of the 1730-1640 Ma Calvert Superbasin (Figs. 2 & 3) and corresponds to a resumption in backarc
108 extension, bimodal magmatism and rift-related sedimentation (Gibson et al., 2016; Jackson et al., 2000;
109 Southgate et al., 2000a). Both NW-SE and NE-SW extensional directions have been proposed for the
110 Calvert Superbasin (Fig. 3) and questions remain about the primary orientation of half-graben hosting the
111 bulk of basin fill. In the McArthur Basin, this includes basaltic rocks of the 1730-1720 Ma Peters Creek
112 Volcanics and Top Rocky Rhyolite (Rawlings et al., 2008) whereas farther afield on the Lawn Hill Platform
113 (Fig. 1a), the Calvert Superbasin hosts basalts of the 1710-1705 Ma Fiery Creek Volcanics (Fig. 3) and
114 fluvial-shallow marine sediments of the 1700-1690 Ma Surprise Creek Formation (Fiery and Prize
115 Supersequences; Southgate et al., 2000). At about the same time that these rocks were being laid down
116 across the Lawn Hill Platform, water depths began to substantially increase farther east in the Mount Isa
117 region so that by 1690 Ma basaltic magmas were being extruded and/or intruded into a deep marine basin
118 filled with turbidites (Black et al., 1998; Foster and Austin, 2008; Gibson et al., 2018; Gibson et al., 2012;
119 Giles et al., 2002; Glikson et al., 1976; Neumann et al., 2009; Rubenach et al., 2008; Scott et al., 2000;
120 Withnall, 1985). Basaltic magmatism continued through to 1655 Ma in the east by which time the
121 Leichhardt Superbasin and lower parts of the Calvert Superbasin had also been intruded farther west by
122 1680-1670 Ma A-type granites (Sybella Granite)(Neumann et al., 2006) and partially unroofed on top-to-
123 the-northeast extensional shear zones (Gibson et al., 2008).

124 With the conclusion of bimodal magmatism at 1655 Ma, the tectonic setting of the Calvert Superbasin
125 transitioned from backarc basin to passive rifted continental margin (Baker et al., 2010; Gibson et al., 2018;
126 Gibson et al., 2012; Neumann et al., 2009) and began to cool and subside, precipitating a marine
127 transgression during the course of which the North Australian Craton was buried beneath a post-rift
128 sequence (Gun Supersequence; Fig. 3) of thin-bedded turbidites, carbonaceous shales, black dolomitic
129 siltstones and carbonate rocks that extended westwards as far as the McArthur Basin (McArthur Group;
130 Fig. 3) and Lawn Hill Platform (Betts et al., 2016; Betts et al., 2006; Gibson et al., 2012; Gibson et al.,
131 2017; Southgate et al., 2013; Withnall and Hutton, 2013).

132 Passive margin conditions persisted until circa 1650 Ma by which time northern Australia was subjected to
133 a further episode of basin inversion (Fig. 3) that lasted until at least 1640 Ma (Riversleigh Tectonic Event)
134 and brought sedimentation in the Calvert Superbasin to a close (Gibson et al., 2018; Gibson et al., 2017;



135 Hinman, 1995; Withnall and Hutton, 2013). Thereafter, the tectonic environment fundamentally changed
136 and crustal extension resumed in a north-south direction (Fig. 3), giving rise to the 1640-1580 Ma Isa
137 Superbasin (Fig. 2) and deposition of a further 6-8 km of sandstone, carbonaceous shales, and dolomitic
138 siltstones (Riversleigh and Term Supersequences) in fault-bounded basins predominantly oriented ENE-
139 WSW (Bradshaw et al., 2000; Bradshaw et al., 2018; Gibson et al., 2020; Gorton and Troup, 2018). Despite
140 the resumption in crustal extension, basaltic rocks are absent and, save for a few tuff beds, there was no
141 corresponding resurgence in felsic magmatism until after the Isa Orogeny had concluded at ca. 1590-1580
142 Ma, some 50-60 Ma later (Black and McCulloch, 1990; Gibson et al., 2018; Withnall and Hutton, 2013).
143 The absence of any significant magmatism is in stark contrast to the two older superbasins, leading some
144 researchers to conclude that the Isa Superbasin represents a sag basin, albeit one periodically punctuated
145 by crustal extension (Betts et al., 2003; Betts et al., 2006), whereas others have argued for deposition in a
146 foreland setting (McConachie and Dunster, 1996), pull-apart basin (Scott et al., 1998; Scott et al., 2000;
147 Southgate et al., 2000a) or syn-orogenic basin in which extension was facilitated by orogen-parallel strike-
148 slip faulting and lateral extrusion of continental crust (Gibson et al., 2020; Gibson et al., 2017). This episode
149 of orogenesis concluded at ca. 1590 Ma (Gibson et al., 2020) or possibly as late as 1580 Ma (Pourteau et
150 al., 2018) before being followed by further crustal extension and successive episodes of pluton-enhanced
151 low pressure-high temperature metamorphism at 1560-1540 Ma and 1520-1490 Ma (Duncan et al., 2011;
152 Foster and Rubenach, 2006; Rubenach et al., 2008). Granitic rocks associated with this late metamorphism
153 have both A- and S-type compositions and are mainly to be found in the east where they are demonstrably
154 of post-tectonic origin, truncating and cutting across folds and axial plane fabrics produced during the Isan
155 Orogeny (Foster and Austin, 2008; Giles et al., 2006; Page and Sun, 1998; Pollard and McNaughton, 1997;
156 Pollard et al., 1998; Withnall and Hutton, 2013).

157 With the conclusion of granitic magmatism at 1500 Ma, much of northern Australia was uplifted and eroded
158 before being buried again beneath younger rocks of the 1490-1450 Ma South Nicholson Basin (Sweet,
159 2017). This Mesoproterozoic basin directly overlies the Isa Superbasin in areas to the west and north of the
160 Lawn Hill Platform (Fig. 1a) and has recently been the subject of a deep seismic reflection study (Carr et
161 al., 2019). Although the seismic data were primarily acquired with a view to better understanding the
162 geometry, thickness and lateral dimensions of this younger basin (Fig. 4), they also serve as a window on
163 the deeper subsurface geology all the way down to crystalline basement and beyond (Carr et al., 2019),
164 thereby providing an opportunity to compare basin architecture in the older sequences below this basin with
165 the results of previous seismic reflection surveys and across a greatly expanded geographical area
166 (Bradshaw et al., 2018; Bradshaw and Scott, 1999; Gibson et al., 2016; McConachie et al., 1993; Scott et
167 al., 1998). These previous seismic reflection surveys highlighted the asymmetric nature of faulting and
168 basin development across the Lawn Hill Platform but differed in respect to basin history and evolution, and
169 more particularly the record of basin inversion and its tectonic drivers (Scott et al., 1998; Gibson et al.,
170 2016; see also Betts et al., 2004). By virtue of the increase in seismic coverage, these issues have become
171 more amenable to investigation and it is to these aspects of basin history and evolution in northern Australia
172 that we now turn.

173 **Seismic record of basin formation and inversion in northern Australia**

174 Survey lines for seismic reflection data acquired across the Lawn Hill Platform and already in the public
175 domain are shown in Figure 5. Most of these are legacy lines dating back to the late 1980s and early 1990s
176 (Burketown Survey, Comalco)(McConachie et al., 1993) and for which reprocessed data became available
177 in 2014 (Armoury Energy). Other lines (Fig. 6a & 6b) were acquired by the minerals industry (Teck
178 Resources, 2011) or minerals industry in collaboration with state and federal Governments (Zinifex,
179 Geological Survey of Queensland and Geoscience Australia, 2006), interpretations of which can be found
180 in several publications and Government records (Bradshaw et al., 2018; Bradshaw and Scott, 1999; Gibson



181 et al., 2017; Gibson et al., 2016; Krassay et al., 2000b; Scott et al., 1998; Southgate et al., 2000b). Results
182 and interpretations of the more recent 2017 South Nicholson Basin survey (Fig. 4) were published jointly
183 by Geoscience Australia and the geological surveys of Queensland and the Northern Territory (Carr et al.,
184 2019) although their interpretation of geology beneath the Carrara Sub-basin (Fig. 4) is not exactly the same
185 as the one presented here, in part owing to uncertainties in extrapolating stratigraphy from existing seismic
186 lines into areas of little or no outcrop or exploratory drilling. A few rare outcrops of basement schist and
187 Carrara Range Group rocks intruded by 1725 Ma Top Rocky Rhyolite (Jackson et al., 2000; Rawlings et
188 al., 2008) are known from the southern Carrara Range immediately north of seismic line 017GA-SN1 but
189 otherwise older parts of the regional stratigraphy are not well exposed, including basaltic rocks (Mitchiebo
190 Volcanics) long thought to be correlative of the Eastern Creek Volcanics in the Leichhardt Superbasin (Fig.
191 3). In a further departure from previously published interpretations of existing seismic data (Gibson et al.,
192 2017), the Calvert and Isa superbasins are both thought here to comprise discrete syn- and post-inversion
193 sedimentary fractions (Fig. 3). These broadly conform with the sedimentary units or supersequences
194 previously identified at the top of each superbasin (Bradshaw et al., 2000; Bradshaw et al., 2018; Domagala
195 et al., 2000; Krassay et al., 2000a; Krassay et al., 2000b; Southgate et al., 2000a) and have an important
196 bearing on basin evolution, and more particularly on the timing and duration of the basin inversion events
197 that brought successive basin cycles to a close. These and other differences with previously published
198 interpretations can be illustrated with a few well-chosen survey lines and there is no need to include
199 interpretations of the full seismic dataset. All lines chosen here are composite and make for two orthogonal
200 but not completely continuous transects across the Lawn Hill Platform, Carrara Range and neighbouring
201 Carrara Sub-basin (Fig. 5). For an alternative and slightly different interpretation of these and other lines in
202 the dataset, the reader is referred to Bradshaw and Scott (2009). Bradshaw et al (2018) and Carr et al (2019).

203 **North-south seismic transect across Lawn Hill Platform**

204 This composite transect is made up of several segments (Figs. 6a & 6b) oriented at high angles to the
205 dominant ENE trend of the Isa Superbasin (Fig. 5). Collectively, these segments image a variably inverted
206 southward-thickening sedimentary wedge disrupted by faults and bounded at its top and bottom by major
207 unconformity surfaces. Limited outcrop across the Lawn Hill Platform and ties to cross lines for which oil
208 well stratigraphic data are available (Fig. 5 & 7) would further suggest that the greater part of this wedge
209 comprises rocks of the Calvert and Isa superbasins (Bradshaw et al., 2000; Bradshaw and Scott, 1999;
210 Gorton and Troup, 2018; Scott et al., 1998; Southgate et al., 2000a) and that the Leichhardt Superbasin is
211 either missing or reduced to a thin layer sandwiched between basement and the overlying younger basins
212 (Figs. 6a & 6b). All five supersequences of the Isa Superbasin (Fig. 3) are represented in the seismic
213 sections, with the base of the sequence reaching extending to depths of 5-6 km along Comalco line 91Bn33-
214 91Bn28 (Fig. 6a). Basin architecture along this line was first described in detail by Bradshaw et al (2000)
215 and their interpretation of inversion-related structures in the River and Term supersequences is not
216 dissimilar to the one presented here. More specifically, as in Bradshaw et al (2000), several inverted normal
217 faults are recognised along this line into which both the River and Term Supersequences manifestly thicken
218 (Fig. 6a); they typically dip northward and even though some of these same faults disrupt and offset
219 sedimentary units in the underlying Calvert Superbasin (Loretta and Prize supersequences, there is no
220 evidence in the seismic section that these structures ever served as growth faults during deposition of the
221 older sedimentary basin. Rather, these north-dipping faults cuts across and postdate stratigraphy in the
222 Calvert Superbasin, and first became active during deposition of the younger Isa Superbasin. No less
223 importantly, both the River and Term supersequences continue southward across the Bluewater Fault Zone
224 into the hangingwall of the Tin Tank Fault where stratigraphy is even more spectacularly inverted (Fig. 6a)
225 and has been deformed into an asymmetric, km-scale south-verging antiform (Punjaub Structure). The



226 River and Term supersequences both attain maximum stratigraphic thickness between the Bluewater and
227 Tin Tank fault zones and occupy much of the fold core (Fig. 6a).

228 Conversely, owing to the effects of erosion, the overlying Lawn and Wide supersequences are only partially
229 preserved over the crest of the antiform. Even so, enough survives of both units beneath their Mesozoic
230 cover rocks to show that these two units progressively thinned over the crest of this fold through a
231 combination of onlap and truncation (Fig. 6a), indicating that the Punjaub Structure either already existed
232 by the time these two units were being deposited or was actively growing during their deposition. In either
233 event, and contrary to previous interpretations (Bradshaw et al., 2000), these two units cannot therefore
234 form part of the syn-extensional growth package. Rather, extension in the Isa Superbasin had already come
235 to a close before sedimentation ceased and these two units more rightly belong to the syn-inversion fraction
236 of basin fill. This is the same conclusion reached by Gibson et al (2017) for the Lawn and Wide sequences
237 exposed along seismic line 06GA-M2 in the Century region farther south (see below).

238 It is further evident from the abrupt truncation of older Calvert-age stratigraphy at the base of the River
239 Supersequence in seismic section 91Bn33-91Bn28 (Fig. 6a) that rocks of the Lawn Hill platform were
240 subjected to an earlier phase of basin inversion, uplift, and erosion before sedimentation in the Isa
241 Superbasin had even started (Bradshaw et al., 2000; Bradshaw et al., 2018; Gibson et al., 2020; Gibson et
242 al., 2017; Scott et al., 1998; Southgate et al., 2000b). As much as 1700m of sedimentary section is estimated
243 to have been lost from the Calvert Superbasin during this inversion event (Bradshaw et al., 2000), a
244 significant amount of which may have been redeposited farther south in the Leichhardt River Fault Trough
245 (Fig. 1a) where there was a commensurate influx of quartz sand at or just before 1640 Ma (Southgate et al.,
246 2000b) during the closing stages of the Calvert Superbasin (Gibson et al., 2017). Truncation of the Calvert
247 Superbasin beneath the River Supersequence is also evident in the Century area (Gibson et al., 2017) and
248 may be further inferred from onlap of the River Supersequence onto older folded rocks of the Calvert
249 Superbasin at depth beneath Mount Caroline (Fig. 6b). Folding of the same amplitude and intensity is not
250 replicated in the overlying River Supersequence and younger sedimentary units, and appears to be confined
251 to the Calvert-age rocks. As elsewhere in the region, the existence of these older structures has largely
252 gone unrecognised owing to extensive overprinting or tightening during the 1620-1580 Ma Isa Orogeny
253 and at least one younger shortening event that postdates the Isa Orogeny and folded all units up to and
254 including the South Nicholson Basin (Fig. 6a). At least some of the folding observed in younger
255 stratigraphic units around the Punjaub Structure may also date from this younger shortening event as is
256 some of the deformation associated with the two northeast-trending periclinal folds (Ploughed Mountain
257 and Mount Caroline) developed northeast of the Century Mine (Fig. 1b). Even more striking are the steep
258 (Boga Fault) and low angle reverse faults that disrupt the core of the Punjaub Structure and cut up section
259 all the way to the Wide Supersequence (Fig. 6a) and may themselves have been folded or reactivated during
260 a younger deformational event.

261 **West-east seismic transect through the Calvert and Isa superbasins**

262 As in the first transect (Fig. 6), seismic sections oriented west-east reveal a wedge-like basin geometry
263 except that units thicken westwards (Fig. 7a & 7b) rather than southward. This is particularly evident in the
264 Isa Superbasin whose constituent lithologies likely occupy a large half-graben that diminishes in depth both
265 laterally and at right angles to the normal faults bounding its southern margin (Fig. 5). As north-dipping
266 structures, these faults are effectively rendered “invisible” in the seismic data. Conversely, growth faults
267 of Calvert age in most seismic sections are well imaged and dip towards the east or northeast (Figs. 7a &
268 7b). They have effected varying amounts of differential thickening and in some instances cut up-section no
269 farther than the Loretta Supersequence at the top of the basin as would be expected of growth faults of this
270 age. A notable exception is the Riversleigh Fault into which stratigraphic units of both the Calvert and Isa



271 superbasins conspicuously thicken (Fig. 8a). This fault was evidently reactivated subsequent to formation
272 of the Calvert Superbasin and continued to be active for a limited time up to and including deposition of
273 the River and lowermost part of the Term supersequences. Thereafter, rocks of the Lawn Hill Platform were
274 buried beneath a post-rift blanket of near constant thickness that comprises the rest of the Term
275 Supersequence, along with an even thicker syntectonic sedimentary package made up of the Lawn, Wide
276 and possibly Doom supersequences (Figs. 3 & 8a). Sedimentary sequences making up this syntectonic
277 package were deposited contemporaneously with basin inversion and commonly thin over the crests of
278 antiformal folds developed in the hangingwall of the Riversleigh Fault and related shortcut thrust fault
279 developed in its footwall (Fig. 8a). Other thrusts, both synthetic and antithetic to the main fault and
280 hangingwall structures, likely developed during the same deformational event, taken here to be the Isa
281 Orogeny. The few large faults cutting upwards through these younger stratigraphic units from deeper levels
282 in the Isa or Calvert superbasins have steeper attitudes and do not appear to be associated with differential
283 thickening, indicating that they too may have formed during the Isa Orogeny or possibly an even younger
284 unrelated tectonic event. In any event, this phase of basin inversion is clearly in addition to the one that
285 predates deposition of the Isa Superbasin and whose main expression in the seismic data is a surface
286 onlapping the older Calvert Superbasin and beneath which rocks of the latter are visibly truncated.

287 **Continuation of west-east seismic transect beneath South Nicholson Basin**

288 Seismic data for the South Nicholson Basin have already been interpreted and published in their entirety
289 (Carr et al., 2019) and this paper is only concerned with parts of the seismic grid (Fig. 4) that connect with
290 existing lines to the east (Fig. 5) and likely share a common basin architecture with the immediately adjacent
291 Lawn Hill Platform. Particularly important in this context is the eastern end of seismic line 017GA-SN1
292 (Fig. 8b) which connects with the Century line (06GA-M2) and extends this west-east transect for some
293 considerable distance westwards (Fig. 4). Older basinal sequences in this region lie buried beneath the
294 South Nicholson Basin and younger cover rocks of Cambrian (Georgina Basin) and Mesozoic age
295 (Carpentaria Basin) and their stratigraphy has largely been determined through the extrapolation of
296 interpreted rock units (Gibson et al., 2017; Gibson et al., 2016) from the existing Century 06GA-M2 line
297 (Fig. 8a). The Isa and Calvert superbasins are both exposed at the surface along line 06GA-M2 but even so
298 interpretations of the subsurface geology along this line and 017GA-SN1 are not completely identical (cf
299 Gibson et al., 2017 and Carr et al., 2019), especially in regard to depth to basement and stratigraphic affinity
300 of the more deeply buried basinal sequences (see also FrogTech Geoscience, 2018). Basement in this study
301 is thought to extend upwards to much higher crustal levels along line 017GA-SN1 than in either Carr et al
302 (2019) or FrogTech Geoscience (2018) and to be directly overlain by a commensurately thinner Leichhardt
303 Superbasin (Fig. 8b). Basin fill in the latter thins westward and, despite disruption by several low-angle
304 faults, can nevertheless be traced for some considerable distance across the seismic section before it pinches
305 out beneath rocks of the unconformably overlying Isa Superbasin and eventually terminates against a major
306 east-dipping normal fault (Fig. 8b). Sedimentary units in the overlying Isa Superbasin have a wedge-like
307 geometry and thicken into this same east-dipping structure which, like the similarly east-dipping
308 Riversleigh Fault, was evidently active at the time this superbasin was deposited (Fig. 8b). Both the River
309 and Term supersequences appear to be represented in this wedge as do correlatives of the Lawn, Wide and
310 Doom supersequences (Fig. 8b). As with their counterparts farther east, the Wide and Doom both thin over
311 the crest of an antiform developed in the hangingwall of the structure and likely constitute the syn-inversion
312 fraction of basin fill. By way of contrast, the River and Term supersequences making up the syn-rift
313 component of basin fill were deposited on an already inverted Leichhardt Superbasin as evidenced by the
314 abrupt truncation of the latter against the base of the overlying River Supersequence (Fig. 8b). Truncation
315 of the Leichhardt Superbasin beneath the Isa Superbasin is no less obvious in the hangingwalls of minor
316 and less intensely inverted faults elsewhere along line 017GA-SN1, lending strong support to the suggestion



317 made repeatedly in this paper that the two older basinal sequences had already undergone at least one phase
318 of uplift and erosion before deposition of the 1640 Ma River Supersequence. Much less clear from line
319 017GA-SN1, owing to the amount of basin inversion involved, is whether the Calvert Superbasin was ever
320 present and simply lost to erosion before sedimentation in the Isa Superbasin commenced. Many of the
321 more important east-dipping faults cut up section all the way to the base of the Isa Superbasin but have only
322 brought about a displacement of the older units and do not appear to be growth faults (Fig. 8b). These faults
323 are either of Calvert or Isa Basin age and possibly predate the much shallower dipping inversion structures
324 that offset all basinal units and continue all the way to the surface. These faults, and some of the steeper or
325 near vertical structures, appear to have been active subsequent to deposition of the South Nicholson Basin
326 which is mildly inverted across them.

327 **North-south seismic sections orthogonal to 017GA-SN1**

328 As a further check on basin geometry and structural architecture to the west of the Lawn Platform, two
329 sections (017GA-SN2 and 017GA-SN4) were selected for interpretation in a direction at a high angle or
330 orthogonal to 017GA-SN1 (Figs. 9a & 9b). With its NW-SE orientation, seismic line 017GA-SN2 cuts
331 across many of the same north or northwest-striking structures imaged in 017GA-SN1, most notably at
332 least one crustal-scale east- or southeast-dipping fault that extends down to the MOHO (Fig. 9a) and is
333 manifestly the same structure responsible for much of the basin inversion observed in the Isa Superbasin.
334 The most obvious difference between the two lines is the thick wedge-like basinal sequence imaged in its
335 hangingwall down to 7.0 seconds TWT. This sequence lies below the interpreted base of the Leichhardt
336 Superbasin in line 017GA-SN1 (Fig. 8b) and either represents an entirely separate older sedimentary
337 package or a continuation of the Leichhardt Superbasin downward to much deeper crustal levels than is
338 immediately apparent in the west-east oriented seismic section. In the absence of independent information,
339 it is not possible to discriminate between these two possibilities except to say that the same package is
340 evidently present in line 017GA-SN1 and corresponds to a zone of non-reflective crust which at a depth of
341 10 kilometres or more seems much too deep for the Leichhardt Superbasin (Fig. 9a) and shares none of the
342 higher amplitude reflectors common to other seismic lines through this basin elsewhere in the Mount Isa
343 region (e.g. 06GA-M3; Gibson et al., 2016). Several low-angle faults on lines 017GA-SN1 and 017GA-
344 SN2 also root downward into this zone (Figs. 8b & 9a) although neither they nor the surfaces bounding the
345 older sedimentary package are particularly conspicuous or maintain their individual character at depth.
346 Rather, all faults and surfaces appear to merge downward into one seismically bland and homogenised
347 region of middle crust more in keeping with expectations for metamorphic basement than the Leichhardt
348 Superbasin. Moreover, because line 017GA-SN1 is probably more closely aligned with lithological strike
349 in the older sedimentary package and its bounding surfaces, their apparent dip in this particular seismic
350 section is close to zero, resulting in surfaces whose traces are subhorizontal and parallel to each other. Only
351 along line 017GA-SN2 is the northern dip of this older package discernible.

352 As with the other two lines across the South Nicholson Basin, 017GA-SN4 (Fig. 9b) encompasses a
353 basement block bounded on its northern side by a near vertical fault. This structure shares the same steep
354 dip as the fault developed along the northern flank of the Punjaub Structure (Fig. 6a) and is possibly the
355 same structural feature. It too serves as the boundary to a wedge of southward-thickening sedimentary rocks
356 whose seismic character (short, high amplitude reflectors) is reminiscent of the along-strike River and Term
357 supersequences. These two sequences are consequently taken here to be part of the Isa Superbasin. They,
358 in turn, are overlain by a sedimentary sequence that likely includes the rest of the Isa Superbasin as well as
359 younger rocks of the South Nicholson and Georgina basins (Fig. 9b).

360 All older sequences are also recognised on the other side of the basement block (Fig. 9b) where they are
361 similarly buried beneath a thin veneer of younger sediments belonging to the South Nicholson and Georgina



362 basins. Basement is pene-planated beneath the Georgina Basin (Fig. 9b) although this likely represents only
363 the latest in a series of uplift and erosion events to have affected this older cratonic block and its overlying
364 sedimentary sequences. Sedimentary sequences on the southern side of the basement block are consistently
365 thinner than their counterparts on the northern side (Fig. 9b) indicating that this block was probably being
366 actively uplifted and eroded before all of the Isa Superbasin had been deposited. Sediment shed from a
367 rising basement block could easily explain the northward-thickening wedge of sediment making up the
368 younger part of the Isa Superbasin identified at the northern end of the seismic section and is in keeping
369 with suggestions made elsewhere that sedimentation and basin inversion in the Isa Superbasin were coeval.
370 Significantly, as in lines 017GA-SN1 and 017GA-SN2, the Leichhardt Superbasin persists in highly
371 attenuated and truncated form, perceptibly thinning up section beneath the overlying Isa Superbasin (Fig.
372 9b).

373 Discussion

374 Extensional basins and their structural architecture both before and after inversion are now reasonably well
375 understood following numerous field studies combined with the results of numerical modelling and
376 sandbox experiments (Cooper et al., 1989; Hayward and Graham, 1989; McClay et al., 2002; McClay and
377 White, 1995; Turner and Williams, 2004). Emphasised in most of these studies is the strongly asymmetric
378 nature of basin fill and the consequences of shortening a sedimentary sequence whose individual unit
379 lengths are all different and increase upward from bottom to top of the section (Hayward and Graham,
380 1989; Lowell, 1995; Turner and Williams, 2004). The net result during shortening is development of an
381 equally asymmetric fold in the hangingwall of the original normal fault which may or may not have been
382 reactivated during the process. This hangingwall fold is one of the most distinctive features of basin
383 inversion and may be regarded as a diagnostic feature, particularly in cases where folding is enhanced by
384 the reactivation of coeval antithetic structures leading to the expulsion of basin fill in opposite directions.
385 Further enhancements of the basic inverted structure may occur where the normal fault locks up early and
386 strain is transferred to a footwall shortcut thrust or taken up by some other structure such as a strike-slip
387 fault (Dooley and McClay, 1997; McClay, 1995; McClay et al., 2002). These and other variations on
388 structural architecture developed during basin inversion (Martínez et al., 2012) are illustrated in Figure 10.
389 All examples are from inverted basins of Mesozoic or younger age but are clearly no less relevant in the
390 case of the older basins described here from northern Australia. Footwall shortcut thrusts have been
391 captured in several of the seismic sections but are conspicuously well developed in the footwalls of the
392 Century (06GA-M2) and Punjaub structures (Figs. 8a & 6b). However, by far the most common and widely
393 imaged structure is the hangingwall antiform (Fig. 10). Moreover, this same structural feature is evident in
394 all sections irrespective of whether they are oriented north-south or west-east, supporting suggestions made
395 elsewhere that there has been more than one episode of basin inversion and that these were imposed on
396 basins that were originally orthogonal to one another. As such, basin inversion affords clues to basin
397 orientation before and after successive episodes of crustal shortening got underway and it is to this topic
398 that we now turn.

399 The Isa Superbasin is best known from the Lawn Hill Platform (Fig. 5) and has been previously interpreted
400 as a sag or foreland basin deformed during a subsequent north-south shortening event identified as the Isan
401 Orogeny (Betts et al., 2003; McConachie et al., 1993; McConachie and Dunster, 1996). More recently, an
402 extensional origin has been proposed for this same basin consistent with seismic data and general thickening
403 of sedimentary units like the River and Term supersequences into normal faults oriented ENE-WSW
404 (Bradshaw et al., 2018; Gorton and Troup, 2018). Antiformal closures developed in the Punjaub Structure
405 and periclinal folds exposed just to its south share the same ENE-WSW trend (Fig. 1b) and likely represent
406 basin inversion structures formed during the same north-south shortening event. However, as already
407 pointed out, the Punjaub Structure is not a simple structure and likely underwent limited folding before or



408 subsequent to the start of deposition in the River and Term supersequences (Gibson et al., 2020). Along
409 with rocks of Calvert age in the core of the Punjaub Structure, these two sequences were deformed during
410 the 1650-1640 Ma Riversleigh Tectonic Event for which a NE-SW shortening direction has been proposed
411 (Gibson et al., 2020; Gibson et al., 2017). As such, shortening during the earlier stages of basin inversion
412 in the Punjaub Structure would have been approximately orthogonal to strike in the Calvert Superbasin and
413 its NW-SE basin-bounding normal faults. Seismic sections oriented parallel to this shortening direction
414 consistently show faults of Calvert age dipping eastwards (e.g. Riversleigh Fault) and several have
415 antiformal structures developed in their hangingwalls (Figs. 8a & 8b) in line with expectations that basin
416 geometry prior to inversion was highly asymmetric and had the form of a westward deepening half-graben.
417 Westward deepening of Calvert-age extensional basins on the Lawn Hill Platform is contrary to the results
418 of earlier geophysical modelling (Betts et al., 2004) indicating that half-graben of this age deepen
419 southwards towards normal faults with NE orientations essentially orthogonal to what is proposed here.
420 However, while faults with this orientation have been previously mapped (Hutton and Sweet, 1982) or have
421 been known to exist in the subsurface for a long time (Krassay et al., 2000a; Scott et al., 1998), it is debatable
422 that they are of Calvert age or exercised any significant control on depositional patterns during this phase
423 of basin formation. They share the same NE to ENE strike as normal faults in the Isa Superbasin and likely
424 belong to the same generation of structures that controlled deposition of the younger sedimentary basin.
425 Importantly, faults of this age exhibit increased amounts of throw southwards which would have been
426 accompanied by commensurate amounts of downward displacement in rocks of the underlying Calvert
427 Superbasin, as captured in seismic images (Fig. 6a) along line 91Bn-28-91Bn33 and the northern flank of
428 Punjaub Structure where the Loretta and Prize supersequences, along with older elements of the Isa
429 Superbasin, have been faulted downward by several kilometres relative to their counterparts across the crest
430 of the fold. This is the same stepped basin geometry picked up in the results of geophysical modelling for
431 the Lawn Hill Platform (Betts et al., 2004) and which, during later crustal shortening, would have produced
432 south-verging folds with the same NE axial direction orientation as periclinal folds now observed at Mount
433 Caroline and Ploughed Mountain (Fig. 1b). It further follows that the NW-SE extensional direction
434 previously proposed for the Calvert Superbasin more likely relates to the younger Isa Superbasin and only
435 came about because erosion across the Lawn Hill Platform during or subsequent to the Isa Orogeny
436 removed much of the younger basin infrastructure leaving behind only the inverted and once more deeply
437 buried rocks of the older basin.

438 West of the Lawn Hill Platform, crystalline basement lies at much shallower crustal depths and may even
439 have been exposed during deposition of the Georgina or South Nicholson basins, forming one or more
440 structural highs over the top of which there is a conspicuous thinning or draping of the younger cover rocks
441 (Fig. 9b). The older Paleoproterozoic-early Mesoproterozoic sequences are similarly notably thinner over
442 basement in this region and the Calvert Superbasin may be entirely missing (Figs. 8b & 9b), either because
443 it was never deposited or was removed by erosion during uplift accompanying the Riversleigh Tectonic
444 Event. The River Supersequence consequently directly overlies on a truncated and westward thinning older
445 sequence taken here to be the Leichhardt Superbasin based on continuity with line 06GA-M2 (Fig. 8a) for
446 which a stratigraphic interpretation has already been published. As with line 06GA-M2 (Fig. 8a), an angular
447 unconformity separates the two sequences (e.g. Fig. 8b), and the Leichhardt Superbasin had likely already
448 been inverted before the River Supersequence was laid down. In keeping with this suggestion, the older
449 sequence has locally been completely eroded away so that the River Supersequence rests directly on older
450 crystalline basement (Fig. 8b). Moreover, even though a significant amount of this uplift and erosion may
451 have been accommodated on reactivated older normal faults, the dominant structures in the seismic images
452 are sub-vertical to steeply dipping and abruptly truncate stratigraphy not only in basement but thick basal
453 sequences developed in their footwalls. These footwall sequences encompass most if not all units of the Isa
454 Superbasin (Figs. 8b & 9b), pointing to either a considerable amount of downward throw to the north on



455 these structures or an equally significant amount of strike-slip displacement. The latter is thought more
456 likely here consistent with the scale and abruptness of truncation and the observation that the faults overall
457 have the character of flower-like structures (Fig. 9b). Either way, it is difficult to avoid the conclusion that
458 basement uplift on these subvertical faults occurred late as these structures displace all units in the Isa
459 Superbasin and cut up-section all the way to the base of the Cambrian. Faults with similarly steep attitudes
460 and character are also evident in north-south oriented seismic sections (Fig. 6) for the northern Lawn Hill
461 Platform (e.g. 91Bn-28; 91Bn-33) and likely belong to the same generation of strike-slip faults.
462 Significantly, they share the same NE to ENE strike and were possibly initiated on older structures dating
463 back to formation of the Isa Superbasin into which they root downward (Fig. 6a).

464 **Basin inversion and implications for Pb-Zn mineralisation**

465 As revealed in seismic sections oriented orthogonal to one another, basin inversion in the north Australian
466 Paleoproterozoic-Mesoproterozoic sequences occurred on more than one occasion and gave rise to a
467 structural architecture not unlike that recorded in basins of much younger age such as the Irish and North
468 seas and North Atlantic petroleum province more generally. No less important in this context are the results
469 of past and recent drilling confirming that northern Australia is prospective for oil and gas (Gorton and
470 Troup, 2018; Jackson et al., 1986; McConachie et al., 1993) thereby amply justifying the case for such
471 comparisons. Further warranting such comparisons is the work of Broadbent et al (1998) who reported that
472 rocks hosting the Century Pb-Zn deposit (Wide Supersequence) are bituminous, since corroborated by more
473 recent studies showing this and other parts of the Isa Superbasin to contain exceptionally high levels of
474 total organic carbon (Gorton and Troup, 2018; Jarrett et al., 2018). Host rocks to the Century deposit include
475 carbonaceous siltstones and dolostones whose carbon content is thought to have transformed these rocks
476 into a suitable reductant during the passage of more oxidising metal-bearing fluids from below. On
477 encountering this reducing environment, a number of catalysed redox reactions ensued during the course
478 of which metal sulphides were precipitated (Broadbent et al., 1998; see also Huston et al., 2006). Other Pb-
479 Zn deposits across the region, including Mount Isa, are thought to have formed through the same process
480 although mineralisation is typically determined to have occurred during basin formation with the metal-
481 bearing fluids transported upwards along normal faults active at the time of sedimentary deposition. Mineral
482 exploration has accordingly often been directed towards the identification of structures and sedimentary
483 sequences formed during the course of basin formation as opposed to those that may have formed during
484 later basin inversion.

485 However, as is now evident from recent seismic interpretations of line 06GA-M2 (Gibson et al., 2017;
486 Gibson et al., 2016), the carbonaceous rocks hosting Century belong to the syn-inversion fraction of basin
487 fill and were deposited at a time of crustal shortening accompanying onset of the Isan Orogeny. There is no
488 evidence that this shortening was accompanied by reactivation of the basin-bounding structure. Instead, as
489 with many normal faults, the Riversleigh Fault dipped too steeply to be easily reactivated and strain was
490 taken up on a footwall shortcut thrust; it rather than the Riversleigh Fault would have served as the better
491 fluid conduit. Interestingly, the Termite Range Fault has some of the same attributes as a footwall shortcut
492 thrust and is widely believed (Broadbent et al., 1998; Yang and Radulescu, 2006) to have been the main
493 fluid conduit for the Century deposit which lies either above or in a minor offshoot immediately adjacent
494 to the master structure. No less importantly, mineralisation is transgressive with respect to stratigraphy and
495 occurred through replacement processes, consistent with the 1575 Ma age reported for this deposit (Carr et
496 al., 2004). This is long after the start of crustal shortening and probable concomitant expulsion of
497 hydrocarbons to higher stratigraphic levels where they would have pooled or been trapped in structures
498 formed during inversion. Alternatively, basin fill at these levels may already have been sufficiently enriched
499 in carbon during the depositional stage. Irrespective of such uncertainties, the metal-bearing fluids migrated
500 into the same structures where they were reduced and forced to give up their Pb and Zn. It seems further



501 likely if the analogy with the petroleum system has any validity that a significant amount of this metal-
502 bearing fluid found its way into the same type of hangingwall structures that are so prospective of oil and
503 gas in the younger inverted basins of the North Atlantic petroleum province. If this is indeed the case, then
504 exploration strategies for sediment-hosted Pb-Zn mineralisation may have to change with exploratory
505 drilling redirected away from former normal faults towards potential structural traps in their hangingwalls.

506 Acknowledgements

507 For the invitation and opportunity to contribute to the special anniversary volume on basin inversion we
508 thank editors, professors Jonas Kley and Piotr Krzywiec. Thanks also to Teck Resources Australia and
509 Pursuit Minerals for permission to publish our interpretation of the Punjaub Structure. Figure 2 was
510 produced on our behalf by Dr Ian Withnall, Geological Survey of Queensland. Seismic reflection data on
511 which this paper depends are available online from their respective data repositories: (Geoscience
512 Australia eCat: <http://pid.geoscience.gov.au/dataset/ga/69674>) and Queensland Geological Survey
513 Burketown survey
514 <https://qdexdata.dnrme.qld.gov.au/GDP/Results?minLong=137.72&maxLong=142.46&minLat=26.3999999992479&maxLat=16.1249999999496>).

517 References

- 518 Andrews, S. J., 1998, Stratigraphy and depositional setting of the upper McNamara Group, Lawn Hill region,
519 Northwest Queensland: *Economic Geology*, v. 93, no. 8, p. 1132-1152.
- 520 Baker, M. J., Crawford, A. J., and Withnall, I. W., 2010, Geochemical, Sm-Nd isotopic characteristics and
521 petrogenesis of Paleoproterozoic mafic rocks from the Georgetown Inlier, north Queensland: implications
522 for relationship with the Broken Hill and Mount Isa eastern succession: *Precambrian Research*, v. 177, p.
523 39-54.
- 524 Betts, P. G., Armit, R. J., Stewart, J., Aitken, A. R. A., Ailleres, L., Donchak, P., Hutton, L., Withnall, I., and Giles, D.,
525 2016, Australia and Nuna: Geological Society, London, Special Publications, v. 424, no. 1, p. 47-81.
- 526 Betts, P. G., Giles, D., and Lister, G. S., 2003, Tectonic environment of shale-hosted massive sulphide Pb-Zn-Ag
527 deposits of Proterozoic northeastern Australia: *Economic Geology*, v. 98, p. 557-576.
- 528 Betts, P. G., Giles, D., and Lister, G. S., 2004, Aeromagnetic patterns of half-graben and basin inversion:
529 implications for sediment-hosted massive sulfide Pb-Zn-Ag exploration: *Journal of Structural Geology*, v.
530 26, no. 6-7, p. 1137-1156.
- 531 Betts, P. G., Giles, D., Mark, G., Lister, G. S., Goleby, B. R., and Ailleres, L., 2006, Synthesis of the Proterozoic
532 evolution of the Mount Isa Inlier: *Australian Journal of Earth Sciences*, v. 53, p. 187-211.
- 533 Betts, P. G., Giles, D., and Schaefer, B. F., 2008, Comparing 1800-1600Ma accretionary and basin processes in
534 Australia and Laurentia: Possible geographic connections in Columbia: *Precambrian Research*, v. 166, no.
535 1, p. 81-92.
- 536 Betts, P. G., and Lister, G. S., 2001, Comparison of the 'strike-slip' versus the 'episodic rift-sag' models for the
537 origin of the Isa Superbasin: *Australian Journal of Earth Sciences*, v. 48, no. 2, p. 265 - 280.
- 538 Bierlein, F. P., Black, L. P., Hergt, J., and Mark, G., 2008, Evolution of pre-1.8 Ga basement rocks in the western Mt
539 Isa Inlier, northeastern Australia--Insights from SHRIMP U-Pb dating and in-situ Lu-Hf analysis of zircons:
540 *Precambrian Research*, v. 163, no. 1-2, p. 159-173.
- 541 Bierlein, F. P., Maas, R., and Woodhead, J., 2011, Pre-1.8 Ga tectono-magmatic evolution of the Kalkadoon-
542 Leichhardt Belt: implications for the crustal architecture and metallogeny of the Mount Isa Inlier,
543 northwest Queensland, Australia: *Australian Journal of Earth Sciences*, v. 58, no. 8, p. 887-915.
- 544 Black, L. P., Gregory, P., Withnall, I. W., and Bain, J. H. C., 1998, U-Pb zircon age for the Etheridge Group,
545 Georgetown region, north Queensland: Implications for relationship with the Broken Hill and Mt Isa
546 sequences: *Australian Journal of Earth Sciences*, v. 45, no. 6, p. 925 - 935.
- 547 Black, L. P., and McCulloch, M. T., 1990, Isotopic evidence for the dependence of recurrent felsic magmatism on
548 new crust formation: An example from the Georgetown region of Northeastern Australia: *Geochimica et*
549 *Cosmochimica Acta*, v. 54, no. 1, p. 183-196.



- 550 Blaikie, T. N., Betts, P. G., Armit, R. J., and Ailleres, L., 2017, The ca. 1740–1710 Ma Leichhardt Event: Inversion of
551 a continental rift and revision of the tectonic evolution of the North Australian Craton: *Precambrian*
552 *Research*, v. 292, p. 75-92.
- 553 Blake, D. H., 1987, *Geology of the Mount Isa Inlier and environs, Queensland and Northern Territory: BMR*
554 *Bulletin*, v. 225, p. 83.
- 555 Bradshaw, B. E., Lindsay, J. F., Krassay, A. A., and Wells, A. T., 2000, Attenuated basin-margin sequence
556 stratigraphy of the Palaeoproterozoic Calvert and Isa Superbasins: the Fickling Group, southern Murphy
557 Inlier, Queensland: *Australian Journal of Earth Sciences*, v. 47, no. 3, p. 599 - 623.
- 558 Bradshaw, B. E., Orr, M. L., Bailey, A. H. E., Palu, T. J., and Hall, L. S., 2018, Northern Lawn Hill Platform: depth,
559 structure and isochore mapping update: *Geoscience Australia Record 2018/47*, 75pp.
- 560 Bradshaw, B. E., and Scott, D. J., 1999, Integrated basin analysis of the Isa Superbasin using seismic, well-log and
561 geopotential data: an evaluation of the economic potential of the northern Lawn Hill Platform: Australian
562 Geological Survey Organisation (now Geoscience Australia) AGSO Record 199/19 (Digital Version).
- 563 Broadbent, G. C., Myers, R. E., and Wright, J. V., 1998, Geology and origin of shale-hosted Zn-Pb-Ag mineralization
564 at the Century Deposit, Northwest Queensland, Australia: *Economic Geology*, v. 93, no. 8, p. 1264-1294.
- 565 Carr, G. R., Denton, G. J., Parr, J., Sun, S.-S., Korsch, R. J., and Boden, S. B., 2004, Lightning does strike twice;
566 multiple ore events in major mineralised systems in northern Australia, *in* Muhling, J., Goldfarb, R.,
567 Vielreicher, N., Bierlein, F., Stumpfl, E., Groves, D. I., and Kenworthy, S., eds., *SEG: Predictive Mineral*
568 *Discovery Under Cover, Extended Abstracts, Volume 33*, p.332-335, Centre for Global Metallogeny, The
569 University of Western Australia, Perth.
- 570 Carr, L. K., Southby, C., Henson, P., Costelloe, R., Anderson, J. R., Jarrett, A. J. M., Carson, C. J., MacFarlane, S. K.,
571 Gorton, J., Hutton, L. J., Troup, A., Williams, B., Khider, K., Bailey, A. H. E., and Fomin, T., 2019, Exploring
572 for the Future: South Nicholson Basin Geological summary and seismic data interpretation. Record
573 2019/21. Geoscience Australia, Canberra.
- 574 Cooper, M. A., Collins, D., Ford, M., Murphy, F. X., and Trayner, P. M., 1984, Structural style, shortening estimates
575 and the thrust front of the Irish Variscides: *Geological Society, London, Special Publications*, v. 14, no. 1, p.
576 167-175.
- 577 Cooper, M. A., Williams, G. D., de Graciansky, P. C., Murphy, R. W., Needham, T., de Paor, D., Stoneley, R., Todd, S.
578 P., Turner, J. P., and Ziegler, P. A., 1989, Inversion tectonics — a discussion: *Geological Society, London,*
579 *Special Publications*, v. 44, no. 1, p. 335-347.
- 580 Domagala, J., Southgate, P. N., McConachie, B. A., and Pidgeon, B. A., 2000, Evolution of the Palaeoproterozoic
581 Prize, Gun and lower Loretta Supersequences of the Surprise Creek Formation and Mt Isa Group:
582 *Australian Journal of Earth Sciences*, v. 47, no. 3, p. 485 - 507.
- 583 Dooley, T., and McClay, K. R., 1997, Analog Modeling of Pull-Apart Basins: *AAPG Bulletin*, v. 81, no. 11, p. 1804-
584 1826.
- 585 Duncan, R. J., Stein, H. J., Evans, K. A., Hitzman, M. W., Nelson, E. P., and Kirwin, D. J., 2011, A New
586 Geochronological Framework for Mineralization and Alteration in the Selwyn-Mount Dore Corridor,
587 Eastern Fold Belt, Mount Isa Inlier, Australia: Genetic Implications for Iron Oxide Copper-Gold Deposits:
588 *Economic Geology*, v. 106, no. 2, p. 169-192.
- 589 Foster, D. R. W., and Austin, J. R., 2008, The 1800–1610 Ma stratigraphic and magmatic history of the Eastern
590 Succession, Mount Isa Inlier, and correlations with adjacent Paleoproterozoic terranes: *Precambrian*
591 *Research*, v. 163, no. 1–2, p. 7-30.
- 592 Foster, D. R. W., and Rubenach, M., 2006, Isograd patterns and regional low-pressure- high-temperature
593 metamorphism of pelitic, mafic and calc-silicate rocks along an east-west section through the Mount Isa
594 Inlier: *Australian Journal of Earth Sciences*, v. 53, p. 167-186.
- 595 Geoscience, F., 2018, North West Queensland SEEBASE® Study and GIS Queensland Geological Record 2018/03.
- 596 Gibson, G. M., and Champion, D. C., 2019, Antipodean fugitive terranes in southern Laurentia: How Proterozoic
597 Australia built the American West: *Lithosphere*, v. 11, no. 4, p. 551-559.
- 598 Gibson, G. M., Champion, D. C., Huston, D. L., and Withnall, I. W., 2020, Orogenesis in Paleo-Mesoproterozoic
599 Eastern Australia: A response to Arc-Continent and Continent-Continent Collision During Assembly of the
600 Nuna Supercontinent: *Tectonics*, v. 39, no. 2, p. e2019TC005717.



- 601 Gibson, G. M., Champion, D. C., Withnall, I. W., Neumann, N. L., and Hutton, L. J., 2018, Assembly and breakup of
602 the Nuna supercontinent: Geodynamic constraints from 1800 to 1600 Ma sedimentary basins and basaltic
603 magmatism in northern Australia: *Precambrian Research*, v. 313, p. 148-169.
- 604 Gibson, G. M., Henson, P. A., Neumann, N. L., Southgate, P. N., and Hutton, L. J., 2012, Paleoproterozoic-earliest
605 Mesoproterozoic basin evolution in the Mount Isa region, northern Australia and implications for
606 reconstructions of the Nuna and Rodinia supercontinents: *Episodes*, v. 35, no. 1, p. 131-141.
- 607 Gibson, G. M., Hutton, L. J., and Holzschuh, J., 2017, Basin inversion and supercontinent assembly as drivers of
608 sediment-hosted Pb–Zn mineralization in the Mount Isa region, northern Australia: *Journal of the*
609 *Geological Society*, v. 174, no. 4, p. 773-786.
- 610 Gibson, G. M., Meixner, A. J., Withnall, I. W., Korsch, R. J., Hutton, L. J., Jones, L. E. A., Holzschuh, J., Costelloe, R.
611 D., Henson, P. A., and Saygin, E., 2016, Basin architecture and evolution in the Mount Isa mineral
612 province, northern Australia: Constraints from deep seismic reflection profiling and implications for ore
613 genesis: *Ore Geology Reviews*, v. 76, p. 414-441.
- 614 Gibson, G. M., Rubenach, M. J., Neumann, N. L., Southgate, P. N., and Hutton, L. J., 2008, Syn- and post-
615 extensional tectonic activity in the Palaeoproterozoic sequences of Broken Hill and Mount Isa and its
616 bearing on reconstructions of Rodinia: *Precambrian Research*, v. 166, no. 1–4, p. 350-369.
- 617 Giles, D., Betts, P. G., Ailleres, L., Hulscher, B., Hough, M., and Lister, G. S., 2006, Evolution of the Isan Orogeny at
618 the southeastern margin of the Mt Isa Inlier: *Australian Journal of Earth Sciences*, v. 53, p. 91-108.
- 619 Giles, D., Betts, P. G., and Lister, G. S., 2002, Far-field continental back-arc setting for the 1.8-1.67 Ma basins of
620 north-east Australia: *Geology*, v. 30, p. 823-826.
- 621 Giles, D., Betts, P. G., and Lister, G. S., 2004, 1.8–1.5-Ga links between the North and South Australian Cratons and
622 the Early–Middle Proterozoic configuration of Australia: *Tectonophysics*, v. 380, no. 1–2, p. 27-41.
- 623 Glikson, A. Y., Derrick, G. M., Wilson, I. H., and Hill, R. M., 1976, Tectonic evolution and crustal setting of the
624 middle Proterozoic Leichhardt River fault trough, Mount Isa region, northwest Queensland: *BMR Journal*
625 *of Australian Geology and Geophysics*, v. 1, p. 115-129.
- 626 Gorton, J., and Troup, A., 2018, Petroleum systems of the Proterozoic in northwest Queensland and a description
627 of various play types: *The APPEA Journal*, v. 58, no. 1, p. 311-320.
- 628 Hayward, A. B., and Graham, R. H., 1989, Some geometrical characteristics of inversion: *Geological Society,*
629 *London, Special Publications*, v. 44, no. 1, p. 17-39.
- 630 Hinman, M., 1995, Base metal mineralisation at McArthur River: structure and kinematics of the HYC-Cooley
631 Zone: *Australian Geological Survey Organisation Record 1995/5*, 41pp.
- 632 Holcombe, R. J., Pearson, P. J., and Oliver, N. H. S., 1991, Geometry of a Middle Proterozoic extensional
633 decollement in north-eastern Australia: *Tectonophysics*, v. 191, p. 255-274.
- 634 Huston, D. L., Stevens, B., Southgate, P. N., Muhling, P., and Wyborn, L., 2006, Australian Zn-Pb-Ag Ore-Forming
635 Systems: A Review and Analysis: *Economic Geology*, v. 101, no. 6, p. 1117-1157.
- 636 Hutton, L. J., and Sweet, I. P., 1982, Geological evolution, tectonic style and economic potential of the Lawn Hill
637 Platform cover, northwest Queensland: *BMR Journal of Australian Geology and Geophysics*, v. 7, p. 125-
638 134.
- 639 Jackson, M. J., Powell, T. G., Summons, R. E., and Sweet, I. P., 1986, Hydrocarbon shows and petroleum source
640 rocks in sediments as old as 1.7×10^9 years: *Nature*, v. 322, no. 6081, p. 727-729.
- 641 Jackson, M. J., Scott, D. L., and Rawlings, D. J., 2000, Stratigraphic framework for the Leichhardt and Calvert
642 Superbasins: Review and correlations of the pre- 1700 Ma successions between Mt Isa and McArthur
643 River: *Australian Journal of Earth Sciences*, v. 47, no. 3, p. 381-403.
- 644 Jarrett, A. J. M., Cox, G. M., Southby, C., Hong, Z., Palatty, P., Carr, L., and Henson, P., 2018, Source rock
645 geochemistry of the McArthur Basin, northern Australia: Rock-Eval pyrolysis data release. *Record*
646 *2018/24. Geoscience Australia, Canberra.*
- 647 Korsch, R. J., Huston, D. L., Henderson, R. A., Blewett, R. S., Withnall, I. W., Fergusson, C. L., Collins, W. J., Saygin,
648 E., Kositcin, N., Meixner, A. J., Chopping, R., Henson, P. A., Champion, D. C., Hutton, L. J., Wormald, R.,
649 Holzschuh, J., and Costelloe, R. D., 2012, Crustal architecture and geodynamics of North Queensland,
650 Australia: Insights from deep seismic reflection profiling: *Tectonophysics*, v. 572–573, no. 0, p. 76-99.
- 651 Kositcin, N., and Carson, C. J., 2019, New SHRIMP U–Pb zircon ages from the South Nicholson and Carrara Range
652 region, Northern Territory. *Record 2019/09. Geoscience Australia, Canberra.*



- 653 Krassay, A. A., Bradshaw, B. E., Domagala, J., and Jackson, M. J., 2000a, Siliciclastic shoreline to growth-faulted,
654 turbiditic sub-basins: the Proterozoic River Supersequence of the upper McNamara Group on the Lawn
655 Hill Platform, northern Australia: *Australian Journal of Earth Sciences*, v. 47, no. 3, p. 533 - 562.
- 656 Krassay, A. A., Domagala, J., Bradshaw, B. E., and Southgate, P. N., 2000b, Lowstand ramps, fans and deep-water
657 Palaeoproterozoic and Mesoproterozoic facies of the Lawn Hill Platform: the Term, Lawn, Wide and Doom
658 Supersequences of the Isa Superbasin, northern Australia: *Australian Journal of Earth Sciences*, v. 47, no.
659 3, p. 563 - 597.
- 660 Kunzmann, M., Schmid, S., Blaikie, T. N., and Halverson, G. P., 2019, Facies analysis, sequence stratigraphy, and
661 carbon isotope chemostratigraphy of a classic Zn-Pb host succession: The Proterozoic middle McArthur
662 Group, McArthur Basin, Australia: *Ore Geology Reviews*, v. 106, p. 150-175.
- 663 Large, R. R., Bull, S. W., McGoldrick, P. J., Walters, S., Derrick, G. M., and Carr, G. R., 2005, Stratiform and strata-
664 bound Zn-Pb-Ag deposits in Proterozoic sedimentary basins, northern Australia: *Economic Geology* 100th
665 Anniversary Volume, p. 931-963.
- 666 Leach, D. L., Bradley, D. C., Huston, D., Pisarevsky, S. A., Taylor, R. D., and Gardoll, S. J., 2010, Sediment-Hosted
667 Lead-Zinc Deposits in Earth History: *Economic Geology*, v. 105, no. 3, p. 593-625.
- 668 Lowell, J. D., 1995, Mechanics of basin inversion from worldwide examples: Geological Society, London, Special
669 Publications, v. 88, no. 1, p. 39-57.
- 670 Martínez, F., Arriagada, C., Mpodozis, C., and Peña1, M., 2012, The Lautaro Basin: A record of inversion tectonics
671 in northern Chile: *Andean Geology*, v. 39, no. 2, p. 258-278.
- 672 McClay, K. R., 1995, The geometries and kinematics of inverted fault systems: a review of analogue model studies:
673 Geological Society, London, Special Publications, v. 88, no. 1, p. 97-118.
- 674 McClay, K. R., Dooley, T., Whitehouse, P., and Mills, M., 2002, 4-D Evolution of Rift Systems: Insights from Scaled
675 Physical Models: *AAPG Bulletin*, v. 86, no. 6, p. 935-959.
- 676 McClay, K. R., and White, M. J., 1995, Analogue modelling of orthogonal and oblique rifting: *Marine and*
677 *Petroleum Geology*, v. 12, no. 2, p. 137-151.
- 678 McConachie, B. A., Barlow, M. G., Dunster, J. N., Meaney, R. A., and Schaap, A. D., 1993, The Mount Isa Basin-
679 definition, structure and petroleum geology: *APEA Journal*, v. 33, no. 1, p. 237-257.
- 680 McConachie, B. A., and Dunster, J. N., 1996, Sequence stratigraphy of the Bowthorn block in the northern Mount
681 Isa basin, Australia: Implications for the base-metal mineralization process: *Geology*, v. 24, no. 2, p. 155-
682 158.
- 683 McGoldrick, P., Winefield, P., Bull, S., Selley, D., and Scott, R. J., 2010, Sequences, Synsedimentary Structures, and
684 Sub-Basins: the Where and When of SEDEX Zinc Systems in the Southern McArthur Basin, Australia, v.
685 Society of Economic Geologists, Special Publication 15, p. 367-389.
- 686 Neumann, N. L., Gibson, G. M., and Southgate, P. N., 2009, New SHRIMP age constraints on the timing and
687 duration of magmatism and sedimentation in the Mary Kathleen Fold Belt, Mt Isa Inlier: *Australian Journal*
688 *of Earth Sciences*, v. 56, p. 965-983.
- 689 Neumann, N. L., Southgate, P. N., Gibson, G. M., and McIntyre, A., 2006, New SHRIMP geochronology for the
690 western fold belt of the Mount Isa Inlier: developing a 1800-1650 Ma event framework: *Australian*
691 *Journal of Earth Sciences*, v. 53, p. 1023-1039.
- 692 O'Dea, M. G., Lister, G. S., Betts, P. G., and Pound, K. S., 1997a, A shortened intraplate rift system in the
693 Proterozoic Mount Isa terrane, N W Queensland, Australia: *Tectonics*, v. 16, p. 425-441.
- 694 O'Dea, M. G., Lister, G. S., MacCready, T., Betts, P. G., Oliver, N. H. S., Pound, K. S., Huang, W., Valenta, R. K.,
695 Oliver, N. H. S., and Valenta, R. K., 1997b, Geodynamic evolution of the Proterozoic Mount Isa terrain:
696 Geological Society, London, Special Publications, v. 121, no. 1, p. 99-122.
- 697 Page, R. W., and Sun, S. S., 1998, Aspects of geochronology and crustal evolution in the Eastern Fold Belt, Mt Isa
698 Inlier: *Australian Journal of Earth Sciences*, v. 45, no. 3, p. 343-361.
- 699 Pearson, P. J., Holcombe, R. J., and Page, R. W., 1991, Synkinematic emplacement of the middle Proterozoic
700 Wonga Batholith into a midcrustal shear zone, Mount Isa Inlier, Queensland, Australia, in Stewart, A. J.,
701 and Blake, D. H., eds., Detailed studies of the Mount Isa Inlier: Australian Geological Survey Organisation
702 Bulletin 243: Canberra, p. 289-328.



- 703 Pollard, P., and McNaughton, N. J., 1997, U/Pb geochronology and Sm/Nd isotope characterization of Proterozoic
704 intrusive rocks in the Cloncurry district, Mount Isa inlier, Australia. AMIRA P438 Cloncurry Base Metals
705 and Gold Final Report: Section 4, 19pp.
- 706 Pollard, P. J., Mark, G., and Mitchell, L. C., 1998, Geochemistry of post-1540 Ma granites spatially associated with
707 regional sodic-calcic alteration and Cu-Au-Co mineralisation, Cloncurry district, northwest Queensland
708 Economic Geology, v. 93, p. 1330-1344.
- 709 Pourteau, A., Smit, M. A., Li, Z.-X., Collins, W. J., Nordsvan, A. R., Volante, S., and Li, J., 2018, 1.6 Ga crustal
710 thickening along the final Nuna suture: Geology, v. 46, no. 11, p. 959-962.
- 711 Pursuit Minerals, 2017, Pursuit Minerals Limited lists on ASX and immediately commences Bluebush Drilling
712 Program. [http://pursuitminerals.com.au/wp-content/uploads/2017/09/PUR-lists-on-ASX-and-](http://pursuitminerals.com.au/wp-content/uploads/2017/09/PUR-lists-on-ASX-and-Commences-Bluebush-Drilling-Program.pdf)
713 [Commences-Bluebush-Drilling-Program.pdf](http://pursuitminerals.com.au/wp-content/uploads/2017/09/PUR-lists-on-ASX-and-Commences-Bluebush-Drilling-Program.pdf).
- 714 Rawlings, D. J., Sweet, I. P., and Kruse, P. D., 2008, Mount Drummond, Northern Territory. 1:250 000 geological
715 map series explanatory notes, SE 53-12. Northern Territory Geological Survey, Darwin.
- 716 Rubenach, M. J., Foster, D. R. W., Evins, P. M., Blake, K. L., and Fanning, C. M., 2008, Age constraints on the
717 tectono-thermal evolution of the Selwyn Zone, Eastern Fold Belt, Mount Isa Inlier: Precambrian Research,
718 v. 163, no. 1-2, p. 81-107.
- 719 Scott, D. L., Bradshaw, B. E., and Tarlowski, C. Z., 1998, The tectonostratigraphic history of the Proterozoic
720 Northern Lawn Hill Platform, Australia: an integrated intracontinental basin analysis: Tectonophysics, v.
721 300, no. 1, p. 329-358.
- 722 Scott, D. L., Rawlings, D. J., Page, R. W., Tarlowski, C. Z., Idnurm, M., Jackson, M. J., and Southgate, P. N., 2000,
723 Basement framework and geodynamic evolution of the Palaeoproterozoic superbasins of north-central
724 Australia: an integrated review of geochemical, geochronological and geophysical data: Australian Journal
725 of Earth Sciences, v. 47, no. 3, p. 341 - 380.
- 726 Southgate, P. N., Bradshaw, B. E., Domagala, J., Jackson, M. J., Idnurm, M., Krassay, A. A., Page, R. W., Sami, T. T.,
727 Scott, D. L., Lindsay, J. F., McConachie, B. A., and Tarlowski, C., 2000a, Chronostratigraphic basin
728 framework for Palaeoproterozoic rocks (1730-1575 Ma) in northern Australia and implications for base-
729 metal mineralisation: Australian Journal of Earth Sciences, v. 47, no. 3, p. 461 - 483.
- 730 Southgate, P. N., Kyser, T. K., Scott, D. L., Large, R. R., Golding, S. D., and Polito, P. A., 2006, A Basin System and
731 Fluid-Flow Analysis of the Zn-Pb-Ag Mount Isa-Type Deposits of Northern Australia: Identifying Metal
732 Source, Basinal Brine Reservoirs, Times of Fluid Expulsion, and Organic Matter Reactions: Economic
733 Geology, v. 101, no. 6, p. 1103-1115.
- 734 Southgate, P. N., Neumann, N. L., and Gibson, G. M., 2013, Depositional systems in the Mt Isa Inlier from 1800 Ma
735 to 1640 Ma: Implications for Zn-Pb-Ag mineralisation: Australian Journal of Earth Sciences, v. 60, p. 157-
736 173.
- 737 Southgate, P. N., Scott, D. L., Sami, T. T., Domagala, J., Jackson, M. J., James, N. P., and Kyser, T. K., 2000b, Basin
738 shape and sediment architecture in the Gun Supersequence: a strike-slip model for Pb-Zn-Ag ore genesis
739 at Mt Isa: Australian Journal of Earth Sciences, v. 47, no. 3, p. 509 - 531.
- 740 Sweet, I. P., 2017, The geology of the South Nicholson Group, northwest Queensland. Queensland Geological
741 Record 2017/07.
- 742 Thomas, D. W., and Coward, M. P., 1995, Late Jurassic-Early Cretaceous inversion of the northern East Shetland
743 Basin, northern North Sea: Geological Society, London, Special Publications, v. 88, no. 1, p. 275-306.
- 744 Turner, J. P., and Williams, G. A., 2004, Sedimentary basin inversion and intra-plate shortening: Earth-Science
745 Reviews, v. 65, no. 3, p. 277-304.
- 746 Withnall, I. W., 1985, Geochemistry and tectonic significance of Proterozoic mafic rocks from the Georgetown
747 Inlier, north Queensland: BMR Journal of Australian Geology & Geophysics, v. 9, p. 339-351.
- 748 Withnall, I. W., and Hutton, L. J., 2013, Chapter 2: North Australian Craton, *in* Jell, P. A., ed., Geology of
749 Queensland: Brisbane, Geological Survey of Queensland, p. 23-112.
- 750 Yang, J., and Radulescu, M., 2006, Paleo-fluid flow and heat transport at 1575 Ma over an E-W section in the
751 Northern Lawn Hill Platform, Australia: Theoretical results from finite element modeling: Journal of
752 Geochemical Exploration, v. 89, no. 1, p. 445-449.

753



754 **Figure Captions**

755 Figure 1. (a) Simplified geological map for northern Australia showing principal tectono-morphological
756 elements and Pb-Zn mineral deposits (after Jackson et al., 2000). (b) More detailed geological map of
757 periclinal folds developed in inverted stratigraphy of the Isa Superbasin on the Lawn Hill Platform east of
758 Century Mine and seismic reflection lines 06GA-M1 and 06GA-M2 along which these structures are
759 imaged. Figure reproduced with permission under the Creative Commons Attribution 4.0 International
760 Licence: <http://creativecommons.org/licenses/by/4.0/legalcode>. © Commonwealth of Australia
761 (Geoscience Australia) 2020.

762 Figure 2. Map showing presently defined limits of outcropping Leichhardt, Calvert and Isa superbasins
763 across the Mount Isa region. Seismic reflection data indicate that all three basins are variably preserved in
764 the subsurface geology beneath the South Nicholson and Georgina basins and continue northwards into the
765 McArthur Basin and Batten Trough (see Carr et al., 2019). Reproduced with permission: Licensed CC BY
766 version 4.0 © State of Queensland, 2020.

767 Figure 3. Simplified stratigraphic column for Mount Isa region and neighbouring southern McArthur
768 Basin showing three-fold subdivision into Leichhardt, Calvert and Isa superbasins but different
769 interpretations of basin history and tectonic evolution (Betts et al., 2003; Betts and Lister, 2001; Gibson et
770 al., 2016; Southgate et al., 2000a). The Carrara Range Group is shown as part of the lower Tawallah
771 Group and a correlative of the Leichhardt Superbasin based on revised mapping (Rawlings et al., 2008)
772 and recently published geochronological data (Kositcin and Carson, 2019) for the McArthur Basin.

773 Figure 4 Superposition of South Nicholson seismic grid over an anomalously deep gravity low bounded by
774 the Carrara Range (gravity high) to the north of line 17GA-SN1 (after Carr et al., 2019) requiring the
775 presence of less dense rocks at depth such as an unusually thick sedimentary basin and/or large felsic
776 igneous body of batholithic proportions such as observed farther south in the Sybella Granite. Figure
777 reproduced with permission under the Creative Commons Attribution 4.0 International Licence:
778 <http://creativecommons.org/licenses/by/4.0/legalcode>. © Commonwealth of Australia (Geoscience
779 Australia) 2020.

780 Figure 5. Basin and basement architecture for northern Lawn Hill Platform showing main depocentres and
781 fault trends for Isa Superbasin (after Gorton and Troup, 2018). Also shown are various industry seismic
782 survey lines from 1994 (Comalco) and 2011 (Teck Resources) across the Isa Superbasin and adjacent
783 Punjab Structure (P). Yellow lines are for composite image presented in Figures 6-7. Note
784 compartmentalisation of depocentres brought about by interference between the ENE and NW-trending
785 faults; latter are of Calvert age and include older normal faults (e.g. Riversleigh Fault) reactivated as strike-
786 slip structures during crustal extension accompanying formation of the Isa Superbasin. Reproduced with
787 permission: Licensed CC BY version 4.0 © State of Queensland, 2020.

788 Figure 6. North-south oriented transect across northern Lawn Hill Platform made up of selected industry
789 and government seismic sections (Fig. 5) showing predominance of north-dipping normal faults on which
790 there has been successive episodes of basin inversion, leaving behind a legacy of fault reactivation and
791 periclinal folding in (a) Punjab Structure and (b) Mount Caroline and Ploughed Mountain (after Gibson et
792 al., 2017; 2020). Note thinning of River and Term supersequences northward through onlap in (a); the
793 underlying Loretta Supersequence similarly thins northward but is bounded top and bottom by truncated
794 surfaces thought to reflect considerable loss of stratigraphic section by uplift and erosion accompanying the
795 1650-1640 Ma Riversleigh Tectonic Event. Sedimentary patterns point to growth faulting on north-dipping
796 structures during deposition of the Isa, but not underlying Calvert Superbasin whose sequences are merely
797 offset. Bluewater, Boga and Tin Tank Fault names adopted from Bradshaw et al (2018) and industry



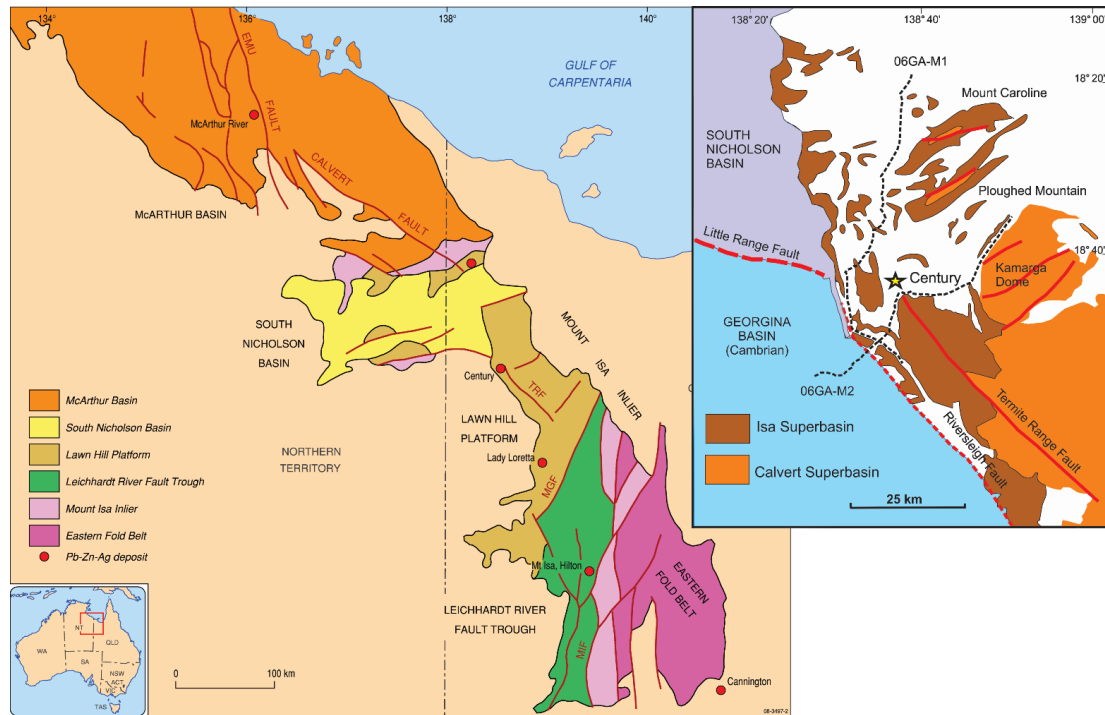
798 (Pursuit Minerals, 2017). In (b) the older sequence had already been folded before the River Supersequence
799 was deposited as evidenced by thinning of the latter over the crests of folds developed in the Calvert
800 Superbasin at deeper levels beneath Mount Caroline. The Calvert Superbasin is in turn separated by an
801 angular unconformity from an even older underlying sequence inferred (Gibson et al., 2017; Gibson et al.,
802 2016) to be the Leichhardt Superbasin. Colour coding is same as Figure 3.

803 Figure 7. West-east oriented seismic transects through northern Lawn Hill Platform. Westward thickening
804 of Calvert-age sedimentary units in both (a) and (b) is consistent with growth faulting on east-dipping
805 normal faults which have since been variably reactivated (Isa Orogeny). Conversely, no such growth is
806 evident in the overlying Isa Superbasin whose lithological strike and inversion structures are essentially
807 parallel to the line of section. These units still thicken into the centre of the Isa Superbasin but in a direction
808 orthogonal to normal faults active during its deposition. Such faults, if imaged, would be expected to be
809 flat-lying or have very shallow dips parallel or subparallel to bedding in both sections rendering their
810 recognition very difficult. Some of the disruption to bedding in (b) along line 90Bn-10 may be due to such
811 faults but overall the most obvious structural feature in the section is the broad arching and folding of
812 stratigraphy in the middle of the section consistent with imaging of an inversion fold in longitudinal cross-
813 section.

814 Figure 8. West-east oriented section through (a) Century Mine (06GA-M2) and (b) its western continuation
815 (017GA-SN1) across the South Nicholson Basin and Carrara Sub-basin (Carr et al., 2019). The older basins
816 of Paleo- Mesoproterozoic age are nowhere exposed along line 017GA-SN1 and the only constraint
817 presently available on their stratigraphy and structural architecture west of the Lawn Hill Platform comes
818 from contiguity with the Century line 06GA-M2 for which an interpretation has already been presented
819 (Gibson et al., 2017; Gibson et al., 2016). Particularly noteworthy in line 017GA-SN1 is the westward
820 thinning of the older sequence beneath the Isa Superbasin, and inversion of it and the Isa Superbasin above
821 a major east-dipping structure that also brought basement to much shallower crustal levels. This older
822 sequence is thought to be of Leichhardt age and has been visibly truncated around the crest of the inversion
823 structure such that the overlying Isa supersequences comes to rest directly on crystalline basement. As in
824 (a), most if not all units of the Isa Superbasin, including the syn-inversion fraction (Lawn, Wide and Doom
825 supersequences), appear to be preserved on the western flank of this inversion structure. An uplifted
826 basement horst block across which basin polarity changes is evident at the western end of the seismic
827 section. The South Nicholson Basin is thinner and shown lying higher than in other recent interpretations
828 (Carr et al., 2019; Geoscience, 2018).

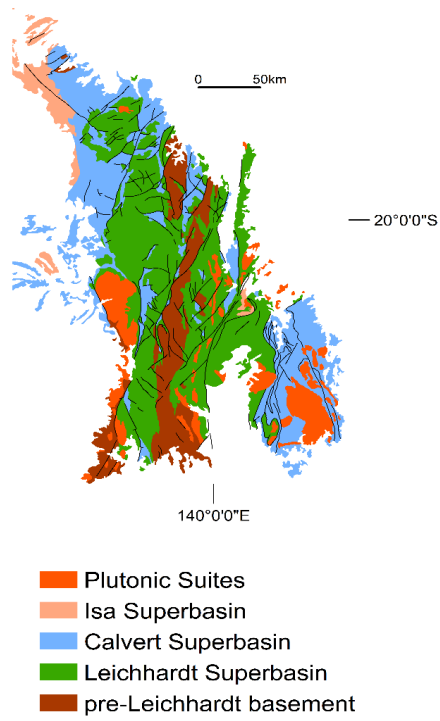
829 Figure 9. North-south oriented seismic sections west of Lawn Hill Platform showing shallow crystalline
830 basement and same basement-rooted inversion structure. Note major basement structure in (a) that cuts
831 downward all the way to the MOHO is probably the same basement structure imaged in (b) and over which
832 all older sedimentary basins have been eroded so that rocks of Cambrian age (Georgina Basin) directly
833 overlie basement (017GA-SN4). Rocks of the South Nicholson have similarly been removed for the crest
834 of this basement block in 017GA-SN4 and, together with rocks of the Isa Superbasin, increase in thickness
835 northwards. The Isa Superbasin is abruptly truncated by the basement structures and other subvertical
836 structures suggestive of a flower structure and late-stage onset of strike-slip faulting at or before deposition
837 of Cambrian Georgina Basin.

838 Figure 10. Basin inversion and resulting styles of structural architecture to be anticipated during crustal
839 shortening (after Martinez et al, 2012; McClay, 1995): (a) early normal fault; (b) harpoon structure from
840 partially inverted normal fault; (c) buttressing; (d) hangingwall is faulted forming hangingwall shortcut; (e)
841 footwall shortcut thrust; (f) folding and truncation of normal fault by younger thrust; (g) thrust ramp above
842 normal fault.



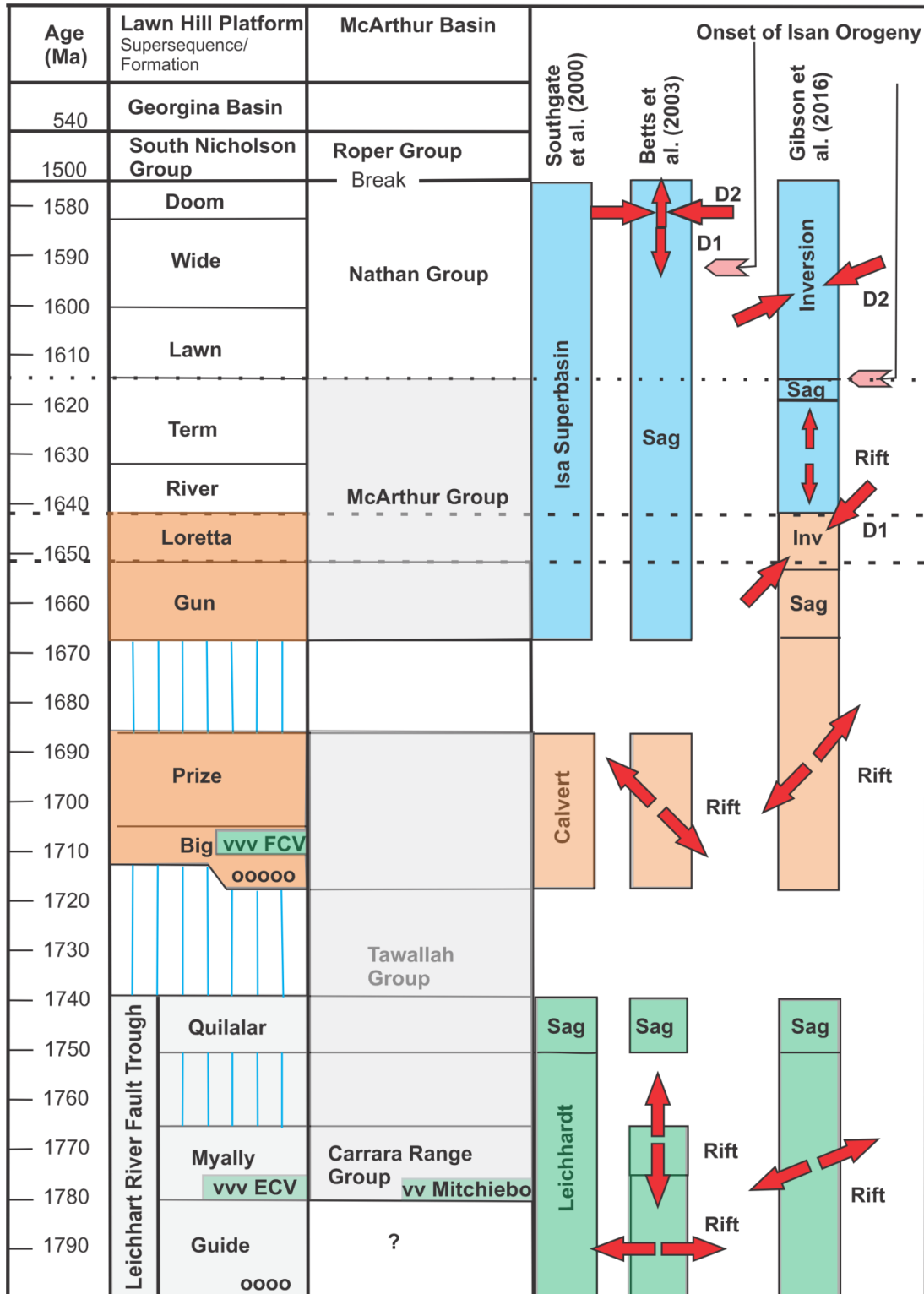
843

844 Figure 1



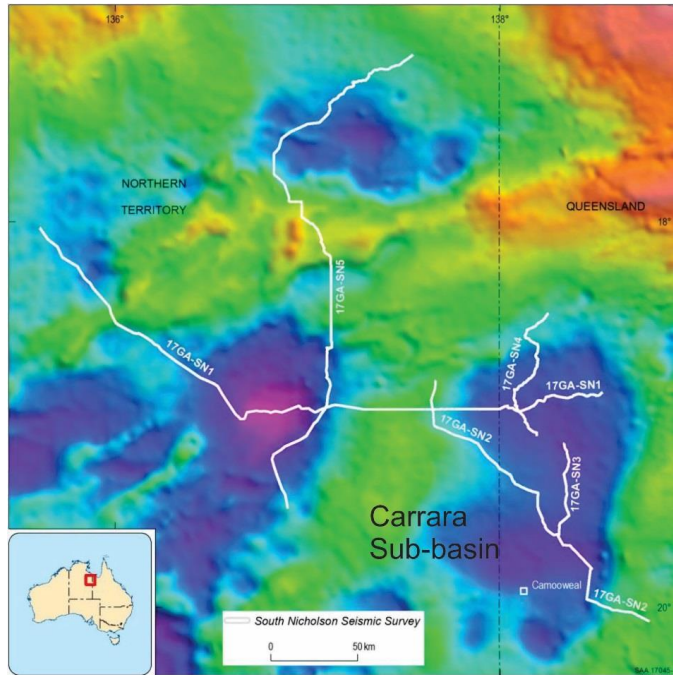
845

846 Figure 2



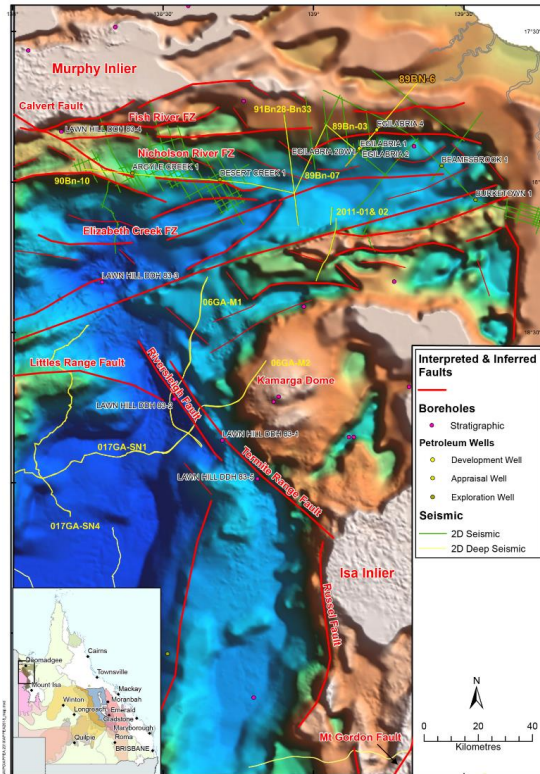


848 Figure 3



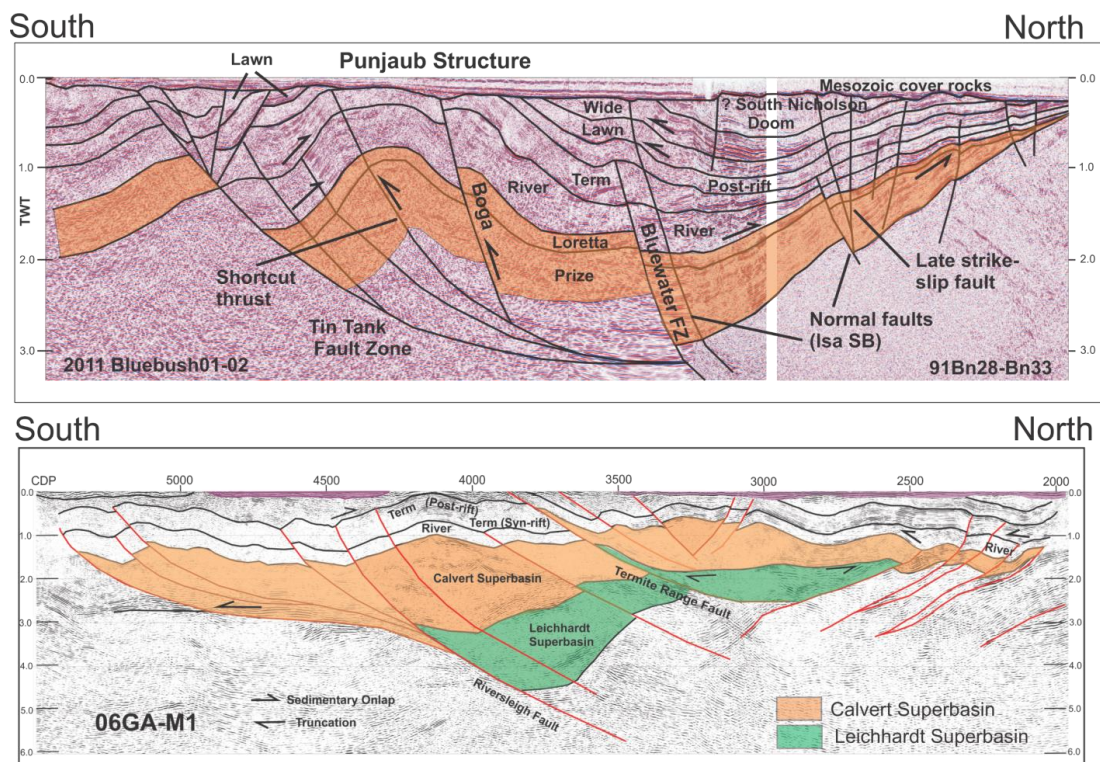
849

850 Figure 4



851

852 Figure 5

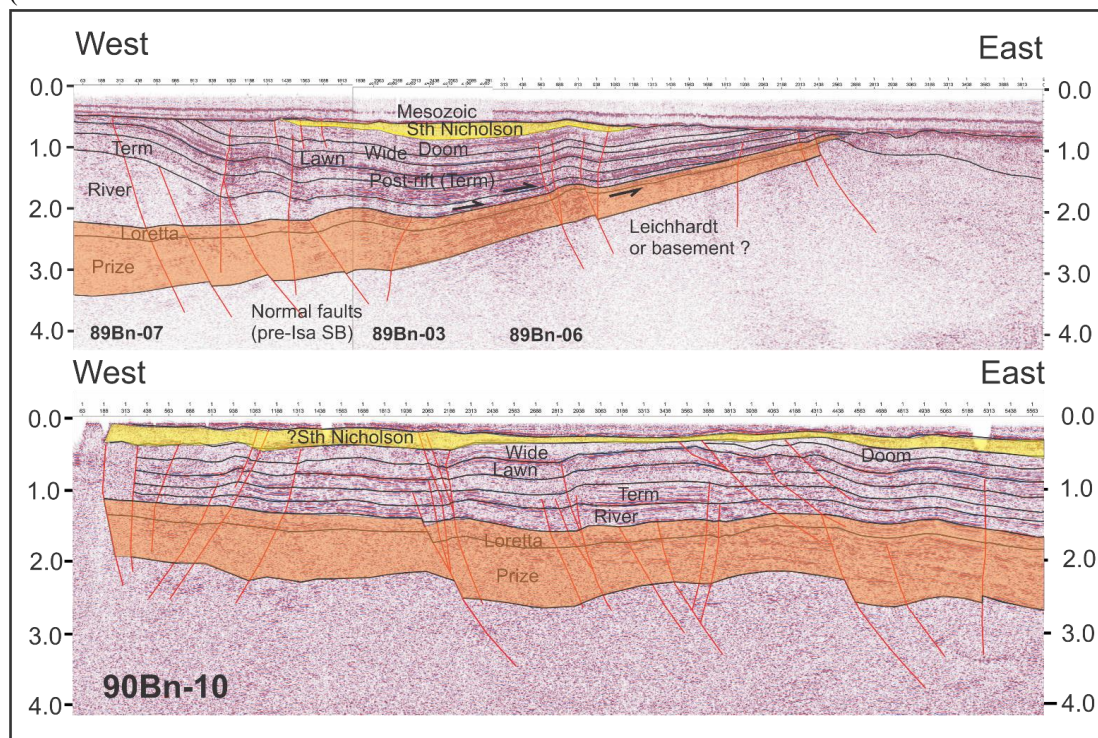


853

854 Figure 6



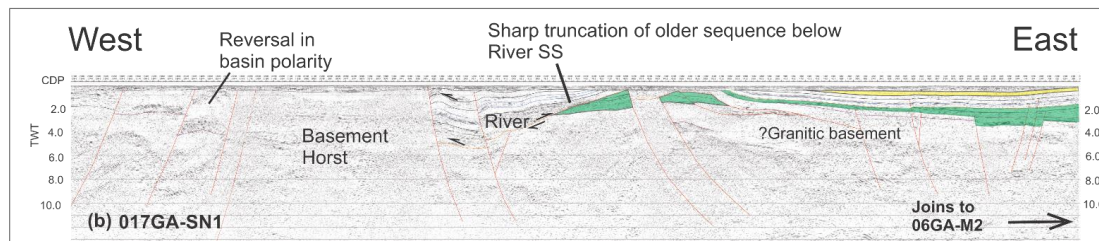
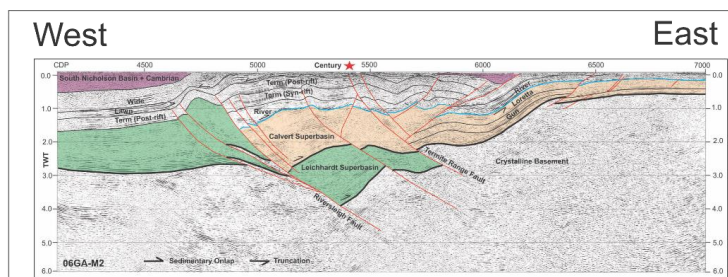
855 (



856

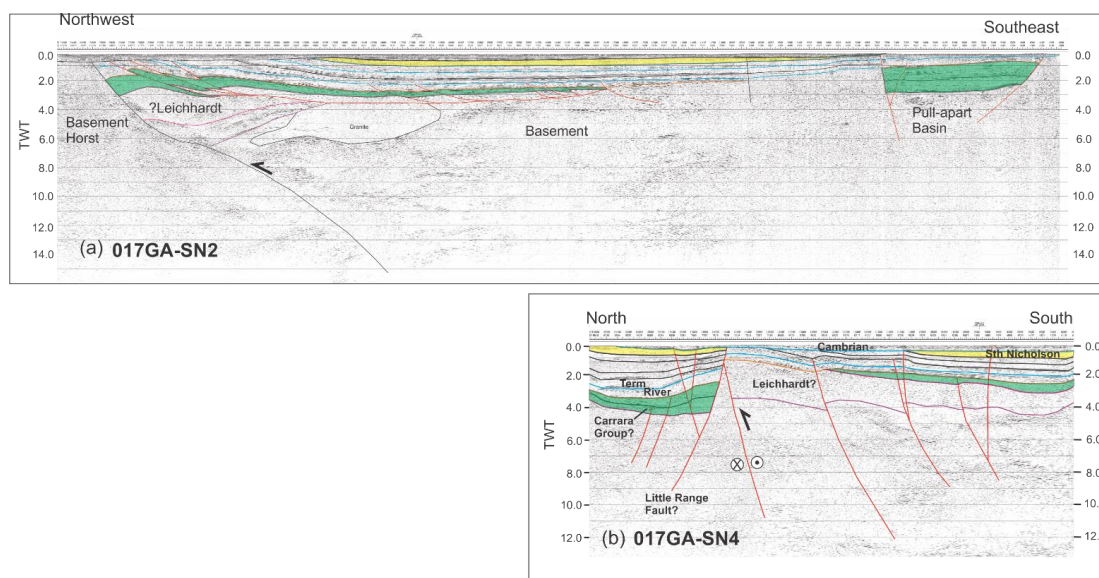
857 Figure 7

858



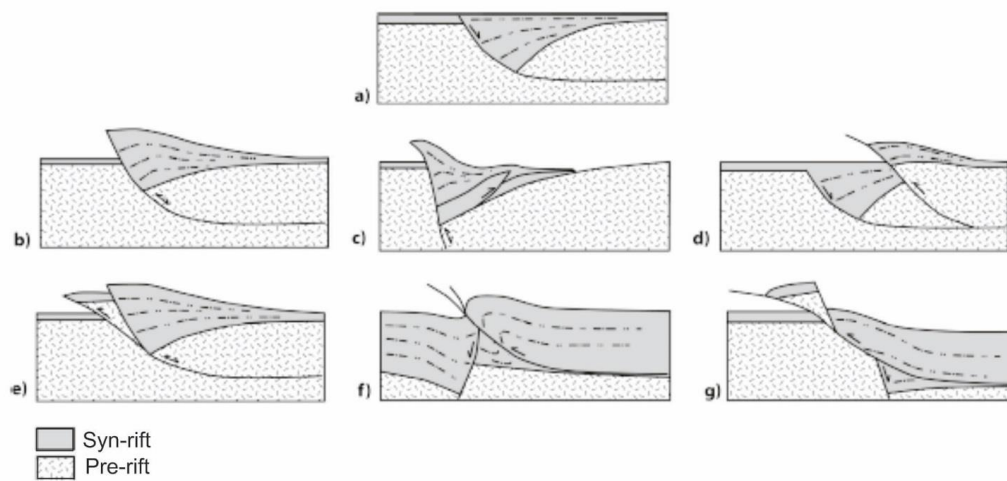
859

860 Figure 8



861

862 Figure 9



863

864 Figure 10